Rotation and Magnetic Activity in a Sample of M-dwarfs

Matthew K. Browning, Gibor Basri, Geoffrey W. Marcy,
Andrew A. West, and Jiahao Zhang

Astronomy Dept, 601 Campbell Hall, UC Berkeley, Berkeley CA 94720-3411

ABSTRACT

We have analyzed the rotational broadening and chromospheric activity in a sample of 121 M-dwarfs, using spectra taken at the W.M. Keck Observatory as part of the California and Carnegie Planet Search program. We find that only six of these stars are rotating more rapidly than our detection threshold of $v\sin i \approx 2.5$ km s^{-1}. Rotation appears to be more common in stars later than M3 than in the M0-M2.5 mass range: we estimate that less than 10% of early-M stars are detectably rotating, whereas roughly a third of those later than M4 show signs of rotation. These findings lend support to the view that rotational braking becomes less effective in fully convective stars. By measuring the equivalent widths of the Ca II H and K lines for the stars in our sample, and converting these to approximate L_{ca}/L_{bol} measurements, we also provide constraints on the connection between rotation and magnetic activity. Measurable rotation is a sufficient, but not necessary condition for activity in our sample: all the detectable rotators show strong Ca II emission, but so too do a small number of non-rotating stars (which we presume may lie at high inclination angles relative to our line of sight). Our data are consistent with a "saturation-type" rotation-activity relationship, with activity roughly independent of rotation above a threshold velocity of less than 4 km s^{-1}. We also find some evidence for a pronounced "gap" in L_{ca}/L_{bol} between a highly active population of stars (which typically are detected as rotators) and another much less active group.

1. INTRODUCTION

Across a broad swath of the Hertzsprung-Russell diagram, rotation and magnetic activity appear to be intimately linked. In stars of spectral types from late F to mid-M, coronal and chromospheric emission – thought partly to trace magnetic heating of the stellar atmosphere – are correlated with rotation (e.g., Noyes et al. 1984, hereafter N84; Delfosse et al. 1998; Pizzolato et al. 2003). Emission in chromospheric Ca II H and K and Hα tends to

rise with increasing rotational velocity, saturating at a threshold velocity that depends upon stellar mass; emission declines somewhat in the most rapid rotators (James et al. 2000). The relationship between rotation and these emission measures is tightened when the rotational influence is expressed using the Rossby number $Ro \sim P/\tau_c$, with P the stellar rotation period and τ_c a typical convective overturning time. This rotation-activity connection is generally thought to reflect the underlying rotational dependence of the magnetic dynamo realized in Sun-like stars.

In such stars, with masses between about 0.35 and 1.3 solar masses, the global dynamo is believed to be seated at the interface layer between the convective envelope and the inner stable region (e.g., Ossendrijver 2003; Parker 1993; Charbonneau & MacGregor 1997). The identification of this region as the likely host of global dynamo action was spurred partly by helioseismology, which revealed that in the Sun this interface is a site of very strong radial shear, called the tachocline (e.g., Thompson et al. 2003). This shear, plus the stable stratification that allows fields to be built up there without quickly becoming susceptible to magnetic buoyancy instabilities (Parker 1975), makes the tachocline the most plausible site where strong toroidal magnetic fields could be amplified and organized, ultimately to emerge at the surface as sunspots. Although the rotational dependence of this process is not yet fully understood, some guidance is perhaps provided by mean field dynamo theory. Such theories parameterize the field generation in solar-like stars as an "$\alpha - \Omega$-dynamo," with the Ω-effect representing the generation of toroidal fields from poloidal by differential rotation, and the α-effect referring to the twisting of fields by helical convection (e.g., Moffatt 1978; Steenbeck, Krause & Radler 1966). In mean field theory, both these effects are sensitive to rotation – the α-effect because it depends upon the helicity of the convection which itself senses the overall rotation rate, and the Ω-effect because more rapidly rotating stars are expected to possess stronger internal angular velocity contrasts. Thus the rotation-activity correlation among stars like the Sun is at least qualitatively consistent with our understanding of the dynamo process.

Toward the low-mass end of the main sequence, our observational and theoretical understanding is far less clear. Mohanty & Basri (2003) argued that a sample of M5-M9 dwarfs exhibited a common "saturation-type" rotation-activity relationship, with the observed chromospheric emission roughly independent of rotation rate above a threshold value. But measuring the rotation rates of M-dwarfs in the "unsaturated" regime of the rotation-activity correlation is difficult, since the corresponding rotational velocities imply modest rotational line broadening that is typically indistinguishable from other effects. Thus it is unclear whether activity in such stars increases gradually with rotation rate, or instead changes more suddenly than in massive stars. Ample observational evidence also indicates that surface magnetic activity is common in the mid-late M-dwarfs, with the fraction of stars

that show chromospheric Hα emission reaching a maximum around M7 (West et al. 2004).

Very recently, the connection between such emission measurements and the underlying magnetic field has begun to be probed directly, using both magnetically sensitive FeH molecular line ratios (Reiners & Basri 2007) and Zeeman Dopper imaging of very rapidly rotating M-stars (Donati et al. 2006). These observations reinforce the view that strong magnetic fields can be built in low-mass stars, and that the fields can possess significant large-scale structure (Donati et al. 2006). Theoretically, a general expectation has been that stars of spectral types later than about M3.5 (with masses less than about 0.35 $M_{\odot}$) might harbor global magnetic dynamos very different from those in more massive stars. Such low-mass stars are convectively unstable throughout their interiors, and so cannot operate an "interface dynamo" precisely like that presumed to act in solar-like stars. Helical convection may still be able to build large-scale magnetic fields, as for instance in the "α^2" mean-field models of Chabrier & Kuker (2006); others have argued that in the absence of organizing shear and a stable layer, the magnetic fields realized in such stars should be mostly on small scales, reflecting the typical size of convective eddies (Durney, De Young & Roxburgh 1993). Numerical simulations have suggested that fully convective stars can build magnetic fields on a variety of spatial scales, and that rotation may still influence the field strengths that are realized (Dobler, Stix & Brandenburg 2006; Browning 2008). Although these models are suggestive, a thorough understanding of how the strength and geometry of dynamo-generated magnetic fields might vary with rotation rate remains elusive.

Part of the problem lies in the difficulty of obtaining reliable estimates of magnetic activity in the M-dwarfs. Most previous studies have employed the chromspheric Hα line as a proxy for magnetic activity, but measurements of that line are fraught with uncertainties (e.g., Cram & Mullan 1979). With increasing activity, Hα first appears in absorption, then fills in the absorption with an emission core, then finally appears in emission. Thus an absence of observable Hα emission can reflect either no activity, or a moderate amount of activity. Chromospheric Ca II emission in the H and and K lines does not share this particular problem, but has proven difficult to probe – it lies blueward of the spectral region where most CCDs have high sensitivity, so has been very difficult to detect in already-faint M-dwarfs. The few M-dwarf studies that have observed the H and K lines have generally done so at low dispersion, since the faintness of these stars would otherwise result in very low signal-noise ratios. Only very recently, with the advent of both 10-m class telescopes and high-resolution spectrographs that are sensitive in the blue, has it become possible to examine the quiescent H and K emission from low-activity M-dwarfs at high spectral resolution, as done by Rauscher & Marcy (2006). Below, we draw extensively upon their data. Such high resolution data is helpful in discerning weak Ca II emission embedded in deep absorption cores (see, e.g., Walkowicz & Hawley 2008).

Additional information about the magnetic fields in M-dwarfs, and their variation with mass and rotation rate, has come from studies of stellar spindown. Stars are born rapidly rotating, arriving on the main sequence with velocities that vary from less than 3 to more than 100 km s^{-1} (Bouvier, Forestini & Allain 1997). They slow over time through angular momentum loss via a magnetized stellar wind (e.g., Skumanich 1972; MacGregor & Brenner 1991). Theoretically, an expectation is that this rotational braking should depend upon the strength of the stellar magnetic field and hence also upon rotation rate (e.g., Weber & Davis 1967; Matt & Pudritz 2008). Observationally, it appears that the time needed for stars to spin down is a strong function of stellar mass (e.g., Barnes 2003). Among the low-mass M-dwarfs, several authors have concluded that the spindown timescale increases with decreasing mass (e.g., Delfosse et al. 1998, Mohanty & Basri 2003). Indeed, most observably rotating M-dwarfs are of spectral types later than M3, suggesting that more massive stars have already spun down to below a detection threshold. The interpretation of these results has been slightly clouded by the small number of stars for which rotation has been measured, and by a systematic bias towards younger stars with decreasing stellar mass (e.g., West et al. 2006). Nonetheless, it has been tempting to ascribe the apparent mass dependence of spindown times to systematic changes in the magnetic field strength or morphology (e.g., Barnes et al. 2003; Durney, De Young & Roxburgh 1993). In a related vein, West et al. (2008) recently used Sloan Digital Sky Survey (SDSS) measurements of Hα emission, in conjunction with a model for galactic dynamical heating of a stellar population, to argue that the "activity lifetime" – the period during which stars exhibit detectable emission – increases significantly between spectral classes M3 and M5. This finding is a further hint that some aspect of the field generation process, or the atmospheric heating mechanism, may change at approximately the mass where stars become fully convective.

These observational and theoretical findings raise a few key questions. One concerns the apparent rarity of measurable rotation in early M-dwarfs: does this paucity of rotators persist at high spectral resolution? And how does the fraction of observed rotators vary with decreasing mass in the M-dwarfs? A second, related question is whether there is any sign of a marked transition in the rotational properties of low-mass stars at the onset of full interior convection – if fully convective stars rotate more rapidly, then this would imply larger spindown times, and so hint at changes in magnetic wind braking. It is already fairly clear that very low mass stars in the late M and L spectral types do tend to rotate more rapidly (Reiners & Basri 2008), but it is uncertain whether this transition to rapid rotation occurs near M3.5, where full convection sets in, or at somewhat lower masses. Quantifying this apparent transition could shed light on whether it is due to a change in the dynamo, or instead to decreasing surface ionization effects that might prevent effective mass and angular momentum loss. The former would probably imply a transition in rotation rates near M3.5,

whereas the latter might be more likely in late-M stars, where the outer layers become increasingly cool and neutral (Mohanty et al. 2002). A final question is whether rotation continues to be linked to magnetic activity in M-dwarfs, as seen in more massive stars (e.g., Skumanich 1972), and in particular if there is any change in this linkage at the mass where stars become fully convective. These questions motivate the work described here.

In this paper, we attempt to measure rotation rates for a largely unbiased sample of 121 K and M-dwarfs, using Keck HIRES data from the California and Carnegie Planet Search Program. Using cross-correlation of the high-resolution stellar spectra with a slowly rotating template, we determine the fraction of stars that rotate more rapidly than about 2.5 km s^{-1} in each spectral type. We analyze the correlation between our measured rotational velocities and chromospheric activity measurements of the same sample (Rauscher & Marcy 2006). Our work is most similar in aims and methods to that of Delfosse et al. (1998), who analyzed the rotation and activity of 118 field M-dwarfs. Indeed, owing to the still small number of low-mass stars accessible to high-resolution spectrographic observations, there is substantial overlap (48 stars) between our target stars and those of Delfosse. However, our sample includes more early-M stars and fewer late-M ones; thus our work can further quantify the apparent rarity of rapid rotators in the early M-dwarfs, and help elucidate the transition in rotation rates throughout the M spectral type. We describe the observational sample and the methods used to measure rotation rates in §2. In §3 we present our rotation analysis, and in §4 we relate these to estimates of chromospheric and coronal activity. We close in §5 with brief comments on the implications of this work.

2. DETERMINING ROTATION RATES

2.1. Observational Sample

We have measured rotation rates in late-type stars using spectra obtained as part of the California and Carnegie Planet Search program. The aims and methods of that program are described elsewhere (e.g., Wright et al. 2004); we here summarize only a few key features of the observational sample and data acquisition. Over the last decade, the Planet Search program has monitored about 2000 stars of spectral types F through M, searching for planets using high-precision radial velocity measurements (Cumming, Marcy & Butler 1999; Butler et al. 2003). Approximately 700 of those stars have been observed using the HIRES spectrometer at the Keck Observatory (Butler et al. 1996), which in its current configuration yields high resolution echelle spectra spanning wavelengths between about 3600 and 8000 Å. The spectral resolution varies depending on the slit width chosen; the sample here has $R \approx 45,000 - 60,000$. The signal to noise ratio also varies but is typically around 60 (Wright

et al. 2004). The data here were all processed using the standard Planet Search pipeline, described by Wright et al. (2004).

From the catalog of Planet Search HIRES spectra, we chose the subset of stars of spectral types M0 or later. We examine only those stars that have been observed since the 2004 upgrade to a three-CCD detector system; this choice allows us to focus mostly on the I-band portion of the spectrum, which is less contaminated by the iodine cell lines used to provide a radial velocity calibration for planet finding. The sample thus defined consists of 510 observations of 124 M-dwarfs. We eliminated three of those stars from consideration because we were unable to reliably analyze their rotation and/or activity using the techniques described below; these three stars were GL 191 (HD 33793), GL 272, and GL 803 (Au Mic). The first two of these have high proper motions that made cross-correlation with a template star difficult; the last (Au Mic) is a young star with a debris disk, which bears little similarity to any of the template stars used in our analysis below. The remaining 121 stars have not been comprehensively examined for rotation, although a few individual targets have been separately discussed elsewhere (Reiners & Basri 2007; Mohanty & Basri 2003; Delfosse et al. 1998).

The sample thus constructed is largely unbiased with respect to rotation rate and chromospheric activity. The stars for the Planet Search program were selected because they were relatively bright (with V magnitudes typically less than 11.5), and because they had no stellar companions within 2". No effort was made to exclude active stars; indeed, some very well known active stars (e.g., V* YZ Cmi) are included. This collection of targets therefore forms a fairly representative sample of M-dwarfs within about 15 pc (Rauscher & Marcy 2006). Such a nearby sample may be implicitly biased toward relatively young objects, since older stars are gradually dynamically heated away from the Galactic disk (e.g., West et al. 2006); thus our sample might be expected to rotate somewhat more rapidly on average than M-dwarfs as a whole.

2.2. Methodology

Measuring the rotation rates of field low-mass stars is challenging for several reasons. Most of these stars appear to rotate so slowly that rotational line broadening is typically small compared to instrumental broadening in moderate-resolution spectra. The threshold rotational velocity above which rotational broadening can be detected of course decreases with increasing spectral resolution, but obtaining high-resolution spectra of faint M-dwarfs is taxing even on the largest of telescopes. Faced with these difficulties, we attempt to extract as much information as possible from the HIRES data available as part of the Planet

Search program, while recognizing that even higher resolution observations would likely reveal rotation in stars that to us appear rotationless.

To measure the rotation rates of stars in our sample, we cross-correlate each stellar spectrum with a high-resolution spectrum of a slowly rotating comparison star. The cross-correlation function (XCF) of the spectra has a minimum at the shift (in pixels) where differences between the spectra are minimized. The width of that minimum – the range of shifts that minimize differences almost as well – is a measure of the average width of features in the two spectra. In effect, the XCF measures the broadening of many different spectral features simultaneously, and so may be less affected by variations in individual lines from star to star. By comparing the widths of the XCF of many different stars versus a common template, we can determine which stars have the broadest lines, and thus are likely the most rapidly rotating. Below a certain threshold rotational velocity (described below), variations from star to star in the width of the XCF will be dominated by random noise, arising either from variations in the instrumental line broadening or from uncertainties in our determination of the XCF width.

For this analysis, we selected a sample of slowly rotating "template" stellar spectra, identified as the stars in each spectral class with the narrowest *auto*-correlation function width. These template spectra were all observed using the "B1" decker on HIRES, yielding a resolution of $R \approx 60,000$; most of the remaining sample consists of observations with the "B5" decker (with $R \approx 45,000$). We then cross-correlated every observed spectra with the template star of its spectral type; for spectral classes for which no "B1" observation was available, we used the template from a nearby spectral class. Because the observations in our sample were taken from the Planet Search program, the stellar spectra are overlaid with lines from an iodine cell placed in the raypath in order to provide a precise radial velocity standard (e.g., Butler et al. 1996). In order to minimize contamination of the XCF determination by the iodine lines, we perform the cross-correlation analysis in the I-band, where the iodine lines are weaker and less numerous than in the R-band. We also chose wavelength regions that are largely free of telluric lines, and which (in the M-dwarfs) are dominated by molecular features. These considerations led us to examine the I-band wavelength regions 6675-6765 Å, 7070-7160 Å, 7530-7565 Å, 7720-7780 Å, and 7870-7930 Å. These regions were divided into 15-Å segments, with a separate cross-correlation analysis performed for each segment; this step was necessary because we did not have an accurate absolute wavelength scale for each observation, so the dispersion varied across each order. Which segments are best for cross-correlation, and which are poor (either because they lack many individual molecular lines or because they are dominated by a single broad feature) varies with spectral type; not all of the above wavelength regions are useful at any one type.

Having calculated the XCF for each of these 15-Å regions, we fit its minimum with a Gaussian profile. Although the choice of a Gaussian profile is arbitrary, an excellent fit to the primary minimum in the XCF can usually be obtained. To automate this process over the $\sim$ 700 spectra considered here, we follow a simple procedure for identifying the feature to be fit: we climb from the minimum of the XCF in both directions until we reach a threshold value that is 95% of a local XCF "continuum." We find that this procedure reliably distinguishes the global minimum of the XCF from many smaller local minima, which arise due to the fairly regular spacing of the molecular lines that dominate M-dwarf spectra. We then store the full-width at half-maximum (FWHM) of the Gaussian fit for each XCF. Outlying FWHMs (which correspond to XCFs for which the Gaussian fit fails) are thrown out; a mean XCF FWHM is calculated for each observation using the remaining FWHM measurements. Finally, we calculate a mean XCF FWHM for each star by averaging over the individual observations. The standard deviation of our individual determinations of the FWHM is typically $\approx$ 0.3 pixels across the $\sim$ 20 different XCFs calculated for each observation; mean FWHM determinations for multiple observations of the same star typically have a standard deviation of 0.1-0.2 pixels.

The measured widths of the XCF for each star are related to the typical width of spectral lines in that star, and hence to its rotational broadening. To calibrate the connection between the XCF widths and rotational velocity, we constructed "spun-up" spectra of our slowly rotating templates, using a standard analytical expression for the rotational broadening (Gray 1992). We convolved these broadened B1-decker observations with a Gaussian profile chosen to mimic the degraded resolution of the B5-decker observations that constitute the bulk of the sample; the width of the Gaussian convolution profile was fixed by comparing ThAr calibration spectra taken using both B1 and B5 deckers. We then cross-correlated these rotationally-broadened templates with the original spectrum (presumed slowly rotating on the basis of its narrow auto-correlation function), and calculated the typical FWHM of the XCF, as described above, as a function of rotational broadening velocity. The resulting calibration of FWHM versus v sin i is shown in Figure 1. This figure indicates that we are not reliably sensitive to rotational velocities less than about 2.5 km s^{-1} : the broadening of the XCF induced by smaller rotational velocities is not significantly greater than the uncertainty in our determination of the FWHMs. Above this threshold, an error of 0.2 pixels in the FWHM determination implies a 1-σ uncertainty of less than 1 km s^{-1} in the v sin i measurement.

Also striking in Figure 1 is the larger FWHM of the M0 template with respect to an M4 template at the same rotation rate. Our other slowly rotating template observations, with spectral classes between M0.5 and M3.5, have typical FWHMs intermediate between these two. This variation in typical line width as a function of spectral class is contrary to the

simple expectation that as molecular lines begin to dominate the spectrum (which occurs with decreasing mass), the typical line width should increase. The variation seen here likely reflects changes in turbulent broadening as a function of mass: decreasing luminosity implies declining convective velocities (with $v_c \propto L_c^{1/3}$, with v_c the typical convective velocity and L_c the luminosity that must be carried by convection), so this translates to less broadening in the least massive stars. A similar decrease in the typical width of cross-correlation profiles with decreasing mass was noted by Delfosse et al. (1998). Likewise, Valenti & Fischer (2005) noted a nearly linear decline in the turbulent macrovelocity with decreasing effective temperature, with v_{turb} declining by about 1 km s^{-1} per 650 K for effective temperatures below 5770 K. This is somewhat steeper than would be expected from the variation in luminosity alone; that scaling would predict, for instance, a drop of about 0.6 km s^{-1} in going from T_{eff} of 5770 to 5120 K (since $v_c \propto T_{eff}^{4/3}$).

By spectral type M4, the broadening in our observations appears to be almost entirely instrumental: applying our cross-correlation technique to ThAr spectra with the B1 and B5 HIRES deckers gave XCF fwhm $\sim$ 5 pixels, comparable to the width of the XCF in our slowly-rotating template stars at that spectral class. This is broadly consistent with extrapolating the Valenti & Fischer (2005) relation for macroturbulent velocities into the low-T_{eff} range probed here; their model would predict zero turbulent broadening below $T_{eff} \approx 3200$ K.

An exception to the trend toward decreasing line width occurs in the very lowest-mass stars in our sample. All six of the M4.5-M6 stars have slightly broader lines (as measured, e.g., by the FWHM of the auto-correlation function) than the slowly rotating M4 template. This may indicate that a small amount of unresolved rotational broadening is present in all the stars later than M4, including those we list here as non-detections (and discuss below).

3. MEASUREMENTS OF ROTATION

Our rotation measurements are collected in Table 1. There we indicate our estimates of v sin i in km s^{-1}, together with identifying information for each star. The most striking feature that emerges from our measurements is how rare measurable rotation is: of the 121 M-dwarfs included in our sample, we detect significant rotational broadening in only six. Another five stars have XCF fwhms that are $\approx 2\sigma$ larger than the typical fwhm (with σ defined here as the typical standard deviation among determinations of the fwhm for multiple observations of one star), but manual inspection suggests that these are still not readily distinguishable from the slowly-rotating template; these stars are noted as "marginal outliers" in Table 1. In practice, we are sensitive to rotational velocities only above ≈ 2.5

km s^{-1}. We have indicated upper limits to v sin i for the remaining stars in Table 1; these are stars whose XCF is indistinguishable from that of the slowly rotating template at the $\approx 2-\sigma$ level.

The distribution of observed rotation rates varies significantly with spectral type. Of the 67 stars in the M0-M3 spectral classes, only 1 (1.5%) had measurable rotation: hip 63510 (with v sin $i \approx 9.5$ km s^{-1}); one other star, HD 95650 shows marginally significant excess broadening, but is still limited to v sin $i \lesssim 2.5$ km s^{-1}). The fraction of measurable rotators appears to increase around M3: of the remaining 54 M-dwarfs in our sample, 5 (9%) had measurable rotation rates, with another 2 showing marginally significant broadening. There are only 6 stars in our sample in the spectral classes M4.5-M6, but 2 of them (hip 37766 and GL 1245b) are significant detections, and a third (GL 83.1) shows a small amount of excess broadening. The fraction of stars observed to rotate above our detection threshold of ≈ 2.5 km s^{-1} is displayed as a function of spectral type in Figure 2. The error bars shown there are purely statistical, and correspond to 1.5-σ errors drawing from a binomial distribution in each mass bin. Because only a few stars later than M3.5 are included in our sample, the error bars on the rotation fractions in that mass range are very large. The conclusion that rotation more rapid than 2.5 km s^{-1} is highly uncommon in the M0-M2.5 spectral types, however, appears to us to be robust. If we instead calculated the error in the rotation fraction by augmenting or subtracting all measured FWHMs by 1σ (with σ again defined not as the standard deviation of the sample, but as a typical standard deviation of the fwhm determinations for multiple observations of the same star), and adopted an arbitrary 2.5 km s^{-1} threshold for detection, the error bars in Figure 2 would be smaller – typically only one or two stars lie within one standard deviation of this cutoff.

The underlying distribution of XCF fwhms for stars in each spectral class, upon which our velocity measurements are based, is shown in Figure 3. The dashed vertical lines in each panel indicate the fwhm of the narrow-lined template in each class, rotationally broadened to v sin i=2.5 km s^{-1}. The detected rotators are generally clear outliers in this distribution. Furthermore, throughout the M1-M3 spectral classes, no stars are particularly close to the $\sim$2.5 km s^{-1} detection limit. There is an overall shift of the average fwhm toward smaller values with decreasing mass, as also realized in Figure 1. This shift is consistent with the overall decline in convective luminosities in going toward decreasing mass.

We believe that the higher fraction of detected rotators in the M3.5-M6 spectral classes, relative to the earlier M subtypes, is not simply a result of the larger fwhm in the early-M slowly-rotating template stars. We also performed cross-correlation of the early-M types with one of the late-M template stars, which had the narrowest auto-correlation fwhm of any star in our sample, in order to determine whether cross-correlation with the broader

M0 template was "hiding" some slow rotators. No new rotation detections in the early-M subtypes emerged from this analysis. In general, we found that cross-correlation with a template of a different spectral type often led to slightly larger values of the XCF fwhm, owing to small mismatches between the two spectra (and to cross-correlation functions that are not fit as well by a simple Gaussian). Typically, the "error" associated with this cross-correlation across different spectral types is less than about 0.5 km s^{-1}. Similarly, we also examined whether our rotational detection threshold in stars later than M4 might be somewhat higher than in M3-M4 stars, owing to the slightly broader lines of the XCF template used for the very lowest-mass stars. Cross-correlating all the M4.5-M6 stars with our M4 template did not significantly change our determinations of rotational velocity.

Our rotation measurements are generally consistent with prior estimates. Our six clear rotation detections are HIP 63510 (v sin $i \approx 9.7$ km s^{-1}), HIP 92403 (GJ 729, 4.0 km s^{-1}), HIP 112460 (GJ 873, 3.5 km s^{-1}), AD Leo (GL 388, 2.7 km s^{-1}), HIP 37766 (GJ 285, 4.6 km s^{-1}), and GL 1245b (7.0 km s^{-1}). Several of the detected stars were also observed by Reiners & Basri (2007) using HIRES in a slightly lower resolution setting; they estimated a v sin i of 4 km s^{-1} for GJ 729, in agreement with our measurement, and find v sin $i \approx 3$ km s^{-1} for AD Leo, also in reasonable accord with our findings. They did not detect rotation in GJ 873, which we find exhibits modest rotational broadening. Delfosse et al. (1998), on the other hand, estimated v sin $i \approx 6.9$ km s^{-1} for the same star; they also found a v sin i of 6.2 km s^{-1} for AD Leo, likewise in appreciable disagreement with our estimate. Although the reasons for this discrepancy are not clear, it may partly stem from the slightly different strategies employed here and in Delfosse et al. (1998) for choosing a slowly-rotating template spectrum: they adopted a common K0 template for comparison with almost all of their stars, whereas we choose a different template for each spectral class. Trial calculations in which we instead used a single M0 template for all spectral classes tended to yield larger velocity estimates, but were still consistent with v sin $i < 4$ km s^{-1} for GJ 873. Our measurement of the rotational velocity of GL 1245b is also identical to that of Reiners & Basri (2007), despite the somewhat different auto-correlation strategies employed here; Delfosse et al. (1998) also found v sin $i = 6.8$ km s^{-1}, consistent with our estimate. HIP 37766 (GJ 285) is the well-known flare star YZ Cmi; both Reiners & Basri (2007) and Delfosse et al. (1998) also published rotation estimates for it, with our measurement consistent with the former (who suggested a value of 5 km s^{-1}) and somewhat smaller than the latter (6.5 km s^{-1}). Finally, the sole star earlier than M3.5 for which we detected measurable rotation, HIP 63510 (GL 494) was also discussed by Beuzit et al. (2004); they quote a measurement of v sin i=9.6 km s^{-1} (determined using the ELODIE spectrograph), in excellent agreement with our own determination.

The near-absence of measurable rotation in the early M spectral classes suggests that

magnetic braking is extremely effective in that mass range. Stars in this mass range are initially rapid rotators, arriving on the main sequence with $v \sin i$ as high as 80 km s^{-1}; even the slowest are typically initially rotating at ~ 10 km s^{-1} (Stauffer & Hartmann 1987). Thus the stars in our sample have slowed by at least a factor of five. A detection $v \sin i$ threshold of ≈ 2 km s^{-1} corresponds to rotation periods of about 16 days at M0 and about 10 days at M3.5 (where we have employed typical mass-radius relationships from, e.g., Ribas 2006).

The near-absence of measurable rotation between M0 and M3 is also consistent with the recent estimates of West et al. (2008), who derived "activity lifetimes" for a large sample of M-dwarfs observed as part of the Sloan Digital Sky Survey. If rotation is correlated with magnetic activity in this mass range, as suggested by, e.g., Delfosse et al. (1998), then the fraction of stars showing magnetic activity should serve as a proxy for the fraction that are rotating more rapidly than some threshold value needed for measurable activity. West et al. (2008) estimate activity lifetimes of about 1 Gyr at spectral type M0, 0.5 Gyr at M1, 2 Gyr at M3, 4 Gyr at M4, and 7 Gyr at M5, suggesting that we should expect to see rotation in 20-40% of stars in the M3-M4 mass range, and in less than 10% of stars from M0-M3. This is very roughly the case: the fraction of stars with measurable rotation is about 10% at M3/M3.5, and 30% in the M4.5-M6 grouping; earlier types show essentially no rotation. This close correspondence provides support for the view that rotation and magnetic activity are intimately linked throughout the mass range probed here. Furthermore, it suggests that the threshold velocity needed for magnetic activity detectable by West et al. (2008) is similar to the minimum velocity measurable in our sample. In the following section, we examine the relation of rotation and activity in more detail.

4. ESTIMATES OF MAGNETIC ACTIVITY

We turn now to estimates of the surface magnetic activity for the stars in our sample, and to the question of whether that activity is linked to the rotation rates we have so far measured. We focus here on the chromospheric emission in the Ca II H and K lines, which have the advantage over Hα that they are much more easily observable in emission if there is any non-radiative heating. This arises partly because these lines are closer to LTE and partly because of the high contrast of the Planck function in the blue. The Ca II H and K emission for our sample has previously been reported by Rauscher & Marcy (2006; hereafter RM06), who published analyses of the H and K equivalent widths (EWs) for all but four of the stars considered here. All the stars we detect as rotators are among the most active emitters in the RM06 compilation; more specifically, all the detected rotators are in the largest 10% of EW measurements, or are noted (in the case of AD Leo and GJ 873) as very

active stars whose Ca emission could not be fit to a Gaussian in the manner used by RM06. Thus all stars rotating above our detection threshold of approximately 2.5 km s^{-1} appear to be active. The converse statement – that all active stars are detectably rotating – is, however, untrue, with the non-rotators in our sample spanning a wide range of Ca II H and K equivalent widths.

To analyze more quantitatively the connection between rotation and magnetic activity in our sample, we have constructed EW measurements analagous to those of RM06, and converted these to values of L_{CaIIH}/L_{bol} and L_{CaIIK}/L_{bol} – the luminosity in each line, normalized by the bolometric luminosity. Unlike the automated EW measurements of RM06, we fit a double Gaussian (to account for the absorption core) to each emission line in each spectrum by hand. Our EW values are computed using the same continuum regions as RM06. The individual line values can be found in West, Zhiang & Marcy (2008, in preparation). The conversion to L_{CaII}/L_{bol} facilitates comparison of activity across different M subtypes: comparing the EW measurement alone can be misleading, since the continuum strength varies by a factor of 50-100 from M0 to M5.5. To construct the L_{Ca}/L_{bol} values, we followed a procedure analogous to that of Walkowicz, Hawley & West (2004) and West, Walkowicz & Hawley (2005), using fluxed spectra with known distances to calibrate the conversions. We measured the absolute flux in the continuum regions used to compute the EWs in the spectra of 21 nearby M-dwarfs. Using the bolometric corrections from Leggett et al. (1996) and Leggett et al. (2001), we computed L_{bol} and the Walkowicz χ (continuum/L_{bol}) for each star. L_{Ca}/L_{bol} values were calculated by multiplying the EW of each star by the average χ value at that spectral type (West & Hawley 2008, in preparation).

The resulting estimates of L_{ca}/L_{bol} are plotted versus v sin i in Figure 4. The H and K luminosity is roughly constant across all the detected rotators. The strongest emission observed is $L_H/L_{bol} \approx 9.0 \times 10^{-5}$ and $L_K/L_{bol} \approx 5.8 \times 10^{-5}$, realized in the star GL 494a (Hip 63510) rotating at v sin $i \approx 9.7$ km s^{-1}. The stars without detectable rotation span two orders of magnitude in L_{ca}/L_{bol}, with the strongest non-rotating emitters possessing normalized Ca luminosities comparable to those of the most rapidly rotating active stars in our sample. Thus measurable rotation (with v sin $i > 2.5$ km s^{-1}) appears to be a sufficient condition for high activity, but not a necessary one.

We presume that some of the highly active stars without measurable rotation might simply be at low inclination angles relative to our line of sight. Of the nine stars in our sample with "saturated" Ca II emission (which we define as log $L_H/L_{bol} > -4.6$, approximately the activity level of the least active rotator), three are not detectably rotating. To estimate roughly how likely it is that these three stars happen to lie at fairly low inclination angles,

we turn to the binomial function

$$P(\text{k out of n}) = \frac{n!}{k!(n-k)!}\, p^k q^{n-k}, \tag{1}$$

which gives the probability of observing k events in n trials, if the probability of an event on each trial is p (and $q = 1 - p$ is the probability of the event not occurring in each trial). For our purposes here, $n = 9$ is the number of active stars observed, and p is the probability that a randomly chosen star will have an inclination angle less than or equal to a chosen angle i; on geometrical grounds, $p = 1 - \cos i$. The binomial formula indicates that we would expect, for instance, to observe three out of nine stars at $i < 45°$ about half the time – i.e., the probability of 3 such events occurring in 9 trials is about $P = 0.50$. Smaller inclination angles occur less frequently: we would expect to see three randomly selected stars (out of 9) at $i < 30°$ only about 11% of the time; only about one time in seventy would we expect to find three stars with $i < 20°$. We can use similar arguments to constrain the possible threshold rotational velocity that might be needed for "saturated" activity: if, for example, all very active stars had intrinsic rotational velocities > 5 km s^{-1}, we would have only about a 3% chance of observing three such stars with $v \sin i < 2$ km s^{-1}; if the threshold velocity needed were instead 4 km s^{-1}, we would see 3 stars at $v \sin i < 2$ km s^{-1} less than 11% of the time. The fact that we *do* see 3 highly active stars without measurable rotation is therefore reasonably strong evidence that the intrinsic rotational velocity needed for such activity is less than 5 km s^{-1} in the mass range studied here.

This relation between rotation and magnetic activity is qualitatively similar to that noted by prior authors who used Hα or X-ray emission as proxies for magnetic activity. Mohanty & Basri (2003) and Delfosse (1998) both found that, in the M-dwarfs, chromospheric emission was consistent with a "saturation-type" rotation-activity correlation, with activity roughly independent of rotation rate above a threshold value; below that threshold, their samples – like ours – showed a wide range of activity levels. Pizzolato et al. (2003), who examined coronal X-ray emission, also found activity in the M-dwarfs to be "saturated" at a value $L_x/L_{bol} \approx 10^{-3.3}$ in all stars with rotation periods shorter than about 10 days – roughly corresponding to our minimum detectable rotational velocity at M3.5. Despite this low threshold for detection, we have likewise found no measurable rotators with particularly low levels of activity, suggesting (as argued above) that any threshold rotational velocity needed for dynamo action must be small indeed.

On a more detailed level, the saturated emission level seen here – with $\log(L_{ca}/L_{bol}) \approx -4.5$ – differs appreciably from the saturation plateau as observed in X-rays and, to a lesser extent, Hα. These tracers are both more luminous (relative to the bolometric luminosity) than the Ca II emission discussed here, typically saturating at $\log(L_x/L_{bol}) \approx -3$ and $\log(L_{H\alpha}/L_{bol})$ between -3.5 and -4. The highest L_{Ca}/L_{bol} achieved in our sample are

comparable to the largest values previously reported (using lower-dispersion spectra) for the flux in the H and K bandpasses, normalized to the bolometric flux – e.g., by Noyes et al. (1984), who quote values of $\log(R'_{hk})$ up to about -4.2 for a sample of more massive stars. The lower level of saturated Ca emission, relative to Hα and X-rays, presumably reflects the fact that less cooling occurs through the Ca II channel than through the Balmer lines, and that the X-ray emission occurs in the corona rather than the chromosphere.

Further information about rotation and activity can be gleaned from Figure 5, which examines the H and K luminosities of our sample as a function of spectral type. The stars for which we have detected rotation are shown there in green. Three main insights emerge from this plot. First, across much of the mass range considered here, there is a clear separation in L_{Ca}/L_{bol} between highly active stars, most of which are detected as rotators, and a significantly less active population of non-rotators. At spectral type M3.5, for instance, the two detectably rotating stars have L_k/L_{bol} and L_H/L_{bol} nearly a factor of ten greater than the most active stars with no measurable rotation. This separation is reminiscent of the "Vaughan-Preston gap" identified in more massive stars (e.g., Vaughan & Preston 1980; Noyes et al. 1984). It could plausibly reflect either two distinct modes of dynamo action, or a range of field strengths in which magnetic spindown is especially rapid (so that few stars linger in that field regime for long).

Second, the mean level of emission among relatively "inactive" stars declines with decreasing mass. The lower L_{Ca}/L_{bol} realized at late types may reflect a decreasing ability of the Ca lines to cool the chromosphere. Interestingly, similar analysis of Hα activity as a function of spectral type in field M-dwarfs (West et al. 2004) has shown no decrease in $L_{H\alpha}/L_{bol}$ at these spectral types: instead, the mean Hα emission remained roughly constant until spectral types M5 or later. This may suggest that the Hα measurements trace primarily the "active" population defined above; in that population, L_{Ca}/L_{bol} also remains fairly constant across the mass range studied here.

Thirdly, although the most active stars are generally detectably rotating, a few are not; some of these stick out from the larger population of inactive non-rotators, and may be good candidates for photometric period determinations or follow-up observations at even higher resolution. At spectral class M2, for instance, the star Gl 569a has L_k/L_{bol} and L_H/L_{bol} about three times larger than the next most active star of that class, yet is not detected as a rotator. (After performing this analysis, we found that GL 569a was claimed by Marcy & Chen 1992 to rotate at 4.0 km s^{-1}; this is inconsistent with our measurement of the XCF FWHM. Very recently, Kiraga & Stepien 2007 measured a photometric rotation period for this star of 13.7 days, which would yield a $v \sin i$ just below our detection threshold even if viewed edge-on.) Other stars that have remarkably high activity but no measurable rotation

include GL 362 (spectral type M3) and GL 406 (M6). As noted above, the existence of a few active stars without measurable rotation is consistent with the expectation that a small number of stars in a random sample will happen to lie nearly pole-on with respect to our line of sight.

All the stars at spectral class M4.5 have fairly high Ca luminosities, and so might also be good candidates for follow-up observation. As noted in §2, we may have no truly non-rotating template star in that mass range to compare with, so our detection threshold in v sin i may be slightly higher than in earlier spectral types. Still, any star rotating more rapidly than 3.0 km s^{-1} in that spectral type should easily have been detected; cross-correlation with narrow-lined templates from other spectral classes did not reveal any such detections. Finally, the most active star in the M0 class was GL 410 (HD 95650); its XCF FWHM was the largest of any star in that subclass, but was still smaller than that expected for a star rotating at 2.5 km s^{-1}, and so we had identified it as a "marginal outlier" in Table 1. It, too, would be an excellent candidate for follow-up observations.

5. SUMMARY AND PERSPECTIVES

We have analyzed the rotation and chromospheric activity of 121 nearby M-dwarfs, using high-resolution spectra taken at Keck as part of the California and Carnegie Planet Search program. We found only six stars rotating more rapidly than our v sin i detection threshold of approximately 2.5 km s^{-1}; in a further 5 stars, we only able to place slightly weaker upper limits on v sin i, ranging from 2.5 to 3 km s^{-1}.

All but two of the detected rotators are of spectral type M3.5 or later, and are therefore probably fully convective, despite the fact that the bulk of our sample (72%) consists of stars in the M0-M3 classes. This finding suggests, though admittedly with still-poor statistics, that rotation more rapid than about 2.5 km s^{-1} is very rare in the early Ms, occurring in less than 10% of stars, and becomes more common with decreasing mass. This, in turn, bolsters the view that the process of rotational braking becomes less effective in fully convective objects – as also suggested, for instance, by observations of rapidly rotating L-dwarfs (e.g., Reiners & Basri 2008), and by studies of the "activity fraction" as a function of stellar mass (West et al. 2008).

We find that rotation is linked to magnetic activity in the following sense: all stars in which we detect rotation are active, but not all active stars are detectably rotating. It is plausible that all the active non-rotating stars happen to lie at low inclination angles relative to our line of sight. Examining the luminosity in the Ca II H and K lines, normalized

to the bolometric luminosity, reveals that over much of the mass range considered here, our sample can plausibly be separated into two fairly distinct populations: one of highly active stars, most of which are detectably rotating, and another of non-rotating stars that generally possess L_{ca}/L_{bol} at least an order of magnitude smaller. The separation between these two groups is analogous to the Vaughan-Preston "gap" claimed in more massive stars (e.g., Vaughan & Preston 1988). The "active" population in our sample has L_h/L_{bol} and $L_{ca}/L_{bol} \approx 10^{-4.5}$, roughly independent of rotation rate, consistent with the "saturation-type" rotation-activity relationship that has previously been claimed in some fully convective stars (e.g., Mohanty & Basri 2003). The level at which L_{ca}/L_{bol} "saturates" in our sample is roughly consistent with prior measurements of the R'_{hk} parameter in more massive stars (e.g., N84), and somewhat lower than the values at which L_x/L_{bol} or $L_{H\alpha}/L_{bol}$ saturate (e.g., Pizzolatto et al. 2003; Delfosse et al. 1998).

Our findings are more similar to those in more massive stars than they might first appear. Rotation is rare in the early M-dwarfs of our sample, but this may be more reflective of the decline in stellar radii with decreasing mass than of fundamentally more effective braking (relative to more massive stars) in that mass range. Our detection limits on $v \sin i$, though representative of the best that can be done using cross-correlation of $R \approx 45000 - 60000$ spectra on a 10-m telescope, still rule out only rather short rotation periods: M-dwarf radii are so small that a $v \sin i$ of 2 km s^{-1} corresponds to a rotation period of about 10 days at M3.5. Thus, a star with a solar-like rotation period (about 28 days) would not be detected here as a rotator.

Our inferences about stellar activity in the M-dwarfs are also surprisingly in line with what has been obtained in more massive stars. The Ca II H and K luminosities L_{ca}/L_{bol} of active, rotating stars in our sample correspond well to the highest values of R'_{HK} noted in prior studies of Sun-like stars (e.g., N84). Furthermore, our threshold period for detection of rotation corresponds fairly well to the period separating young, active stars in the N84 survey from old, less active ones. Put another way, all our detected rotators would, if they were more massive but had the same rotation period, be part of the "active" population in N84's sample; our non-rotators would generally (if similarly converted to greater masses) fall into the solar-like low-activity population in that sample. Probably the most striking difference between our activity measurements and those in more massive stars is the larger spread in L_{Ca}/L_{bol} values we observe. Some of the low-activity, non-rotating stars in our sample have L_{Ca}/L_{bol} as low as $10^{-6.5}$, more than a factor of ten lower than the smallest values of R'_{HK} reported in N84. It is unclear why the chromospheric luminosities of these least active M-dwarfs extend to much lower values than in more massive stars, particularly given that the L_{Ca}/L_{bol} achieved by the *most* active stars appears roughly independent of stellar mass. This may well simply reflect the decreasing efficiency of the Ca II lines as

a cooling channel, as noted above. Another possible explanation is that some of the stars in our sample are rotating much more slowly than any solar-like stars, and that activity continues to be related to rotation period in such slow rotators; testing this possibility will require photometric rotation period measurements for some of the inactive stars that we list as non-rotators.

The implications of our findings for dynamo theory are not entirely clear. On the one hand, there appear to be close analogues between dynamos in low-mass M-dwarfs (some of which are fully convective) and dynamos in more massive stars: both seem to obey some form of rotation-activity relation, both are capable of generating similar maximum chromospheric luminosities (L_{Ca}/L_{bol}), and both may possess fairly distinct active and inactive populations (separated by a "gap" in L_{Ca}/L_{bol}). Furthermore, the rotation period dividing the inactive, slowly rotating stars from their active cousins seems not to depend too strongly upon stellar mass. This latter point may reflect the central role of rotation in dynamo action, together with only modest variations in the convective turnover time τ_c with stellar mass. On the other hand, the fact that measurable rotation seems very rare in early-M stars in our sample – with only 1 M0-M2 star in 70 showing v sin i in excess of 2 km s^{-1} – but fairly common in stars of spectral type M3.5 or later – where 4 stars in 17 are detectably rotating – indicates that *something* about stellar spindown changes near the onset of full convection in stars. Whether that change is due to variations in the strength of dynamo-generated fields, their geometry, their coupling to a stellar wind, or to some yet unforseen effect, remains to be determined.

This work was supported in part by an NSF Astronomy and Astrophysics postdoctoral fellowship (AST 05-02413).

REFERENCES

Barnes, S.A. 2003, ApJ, 586, 464

Beuzit, J.L., Segransan, D., Forveille, T., Udry, S., Delfosse, X., Mayor, M., Perrier, C., Hainaut, M.-C., Roddier, C., & Roddier, F., 2004, A&A, 425, 997

Browning, M.K., 2008, ApJ, 676, 1262

Bouvier, J., Forestini, M., & Allain, S., 1997, A&A, 326, 1023

Butler, R.P., Marcy, G.W., Williams, E., McCarthy, C., Dosanjh, P., & Vogt, S.S., 1996, PASP, 108, 500

Butler, R.P., Marcy, G.W., Vogt, S.S., Fischer, D.A., Henry, G.W., Laughlin, G., & Wright, J.T., 2003, ApJ, 582, 455

Chabrier, G. & Kuker, M., 2006, A&A, 446, 1027

Charbonneau, P., & MacGregor, K.B. 1997, ApJ, 486, 502

Cram, L.E., & Mullan, D.J., 1979, ApJ, 234, 579

Cumming, A., Marcy, G.W., & Butler, R.P., 1999, ApJ, 526, 890

Delfosse, X., Forveille, T., Perrier, C., & Mayor, M. 1998, A&A, 331, 581

Dobler, W., Stix, M., & Brandenburg, A., 2006, ApJ, 638, 336

Donati, J.F., Forveille, T., Cameron, A.C., Barnes, J.R., Delfosse, X., Jardine, M.M., & Valenti, J.A., 2006, Science, 311, 633

Durney, B.R., De Young, B.S., & Roxburgh, I.W., 1993, Sol. Phys., 145, 207

Gray, D.F., 1992, The Observation and Analysis of Stellar Photospheres (2nd ed.; Cambridge: Cambridge Univ. Press)

James, D.J., Jardine, M.M., Jeffries, R.D., Randich, S., Collier Cameron, A., Ferreira, M., 2000, MNRAS, 318, 1217

Kiraga, M., & Stepien, K., 2007, Acta Astronomica, 57, 149 (arXiv:0707.2577)

Leggett, S. K., Allard, F., Berriman, Graham, Dahn, Conard C., & Hauschildt, Peter H., 1996, ApJS, 104, 117

Leggett, S. K., Allard, F., Geballe, T. R., Hauschildt, P. H., & Schweitzer, A., 2001, ApJ, 548, 908

MacGregor, K.B., & Brenner, M., 1991, ApJ, 376, 204

Marcy, G.W., & Chen, G.H., 1992, ApJ, 390, 550

Matt, S., & Pudritz, R.E., 2008, ApJ, 678, 1109

Moffatt, H. K. 1978, Magnetic field generation in electrically conducting fluids (Cambridge, England, Cambridge University Press)

Mohanty, S. & Basri, G., 2003, ApJ, 583, 451

Mohanty, S., Basri, G, Shu, F., Allard, F., & Chabrier, G., 2002, ApJ, 571, 469

Noyes, R. W., Hartmann, L. W., Baliunas, S. L., Duncan, D. K., & Vaughan, A. H. 1984, ApJ, 279, 763

Ossendrijver, M. 2003, Astron. Astrophys. Rev., 11, 287

Parker, E. N. 1975, ApJ, 198, 205

Parker, E. N. 1993, ApJ, 408, 707

Pizzolato, N., Maggio, A., Micela, G., Sciortion, S., & Ventura, P., 2003, A&A, 397, 147

Rauscher, E., & Marcy, G.W., 2006, PASP, 118, 617

Reiners, A., & Basri, G., 2007, ApJ, 656, 1121

Reiners, A., & Basri, G., 2008, ApJ accepted (arXiv:0805.1059)

Ribas, I., 2006, Ap & SS, 304, 89

Skumanich, A. 1972, ApJ, 171, 565

Stauffer, J.R., & Hartmann, L.W., 1987, ApJ, 318, 337

Steenbeck, M., Krause, F., & Radler, K. H. 1966, ZNatA, 21, 369S

Thompson, M. J., Christensen-Dalsgaard, J., Miesch, M. S., & To omre, J. 2003, ARA&A, 41, 599

Valenti, J.A., & Fischer, D.A., 2005, ApJS, 159, 141

Vaughan, A.H., & Preston, G.W., 1980, PASP, 92, 385

Walkowicz, L.M., Hawley, S.L., & West, A.A., 2004, PASP, 116, 1105

Walkowicz, L.M., & Hawley, S.L., 2008, AJ, submitted

Weber, E.J. & Davis, L., 1967, ApJ, 148, 217

West, A. A., et al., 2004, AJ, 128, 426

West, A.A., Walkowicz, L.M., & Hawley, S.L., 2005, PASP, 117, 706

West, A.A., Bochanski, J.J., Hawley, S.L., Cruz, K.L., Covey, K.R., Silvestri, N.M., Reid, I.N., & Liebert, J., 2006, AJ, 132, 2507

West, A.A., Hawley, S.L., Bochanski, J.J., Covey, K.R., Reid, I.N., Dhital, S., Hilton, E.J., & Masuda, M., 2008, AJ, 135, 785

Wright, J.T., Marcy, G.W., Butler, R.P., & Vogt, S.S., 2004, ApJS, 152, 261

Table 1. Summary of Rotation and Activity Measurements

GL	HIP/other	Type	L_h/L_{bol}	L_k/L_{bol}	$v \sin i$ (km/s)
		Detections			
285	37766	M4.5	5.0e-05	3.3e-05	4.6
388	ADLeo	M3	3.3e-05	2.2e-05	2.7
494a	63510	M0.5	9.0e-05	5.8e-05	9.7
729	92403	M3.5	2.9e-05	1.9e-05	4.0
873	112460	M3.5	4.1e-05	2.7e-05	3.5
1245b	-	M5.5	4.3e-05	2.9e-05	7.0
		Marginal Outliers			
27.1	3143	M0.5	6.9e-06	4.4e-06	< 3.0
48	4856	M3	2.6e-06	1.8e-06	< 2.5
83.1	-	M4.5	2.0e-05	1.3e-05	< 2.5
410	53985	M0	4.0e-05	2.6e-05	< 2.5
3804	67164	M3.5	1.4e-06	9.5e-07	< 2.5
		Non-detections			
2	428	M1	1.4e-05	9.3e-06	< 2.5
1	439	M1.5	1.4e-06	1.0e-06	< 2.5
15	1475	M1.5	2.1e-06	1.5e-06	< 2.5
1009	1734	M1	1.4e-05	9.5e-06	< 2.5
26	-	M2.5	2.6e-06	1.9e-06	< 2.5
54.1	5643	M4.5	1.1e-05	8.5e-06	< 2.5
70	8051	M2	5.2e-06	3.9e-06	< 2.5
3126	G244-047	M3	3.1e-06	2.2e-06	< 2.5
87	10279	M1.5	2.6e-06	2.0e-06	< 2.5
96	11048	M0.5	1.4e-05	1.0e-05	< 2.5
105b	-	M4	9.6e-07	6.9e-07	< 2.5
109	12781	M3	2.3e-06	1.8e-06	< 2.5
173	21556	M1.5	3.8e-06	2.8e-06	< 2.5
179	22627	M3.5	3.0e-06	2.2e-06	< 2.5
180	22762	M2	3.4e-06	2.5e-06	< 2.5
3325	23512	M3	2.0e-06	1.5e-06	< 2.5
192	24284	M2	2.5e-06	1.9e-06	< 2.5

Table 1—Continued

GL	HIP/other	Type	L_h/L_{bol}	L_k/L_{bol}	$v \sin i$ (km/s)
205	25878	M1.5	1.6e-05	1.1e-05	< 2.5
3356	G097-054	M3.5	1.8e-06	1.3e-06	< 2.5
212	26801	M0.5	2.0e-05	1.5e-05	< 2.5
213	26857	M4	1.0e-06	7.4e-07	< 2.5
3378	G192-13	M3.5	2.5e-06	1.8e-06	< 2.5
none	29052	M4	1.2e-06	9.2e-07	< 2.5
226	29277	M2	3.4e-06	2.5e-06	< 2.5
229a	29295	M0.5	1.4e-05	9.9e-06	< 2.5
250b	-	M2	5.9e-06	4.2e-06	< 2.5
251	33226	M3	1.1e-06	8.6e-07	< 2.5
273	36208	M3.5	1.2e-06	9.1e-07	< 2.5
1097	36338	M3	1.6e-06	1.1e-06	< 2.5
277.1	36834	M0.5	5.1e-06	3.5e-06	< 2.5
3459	37217	M3	1.5e-06	1.1e-06	< 2.5
2066	40501	M2	3.7e-06	2.9e-06	< 2.5
317	-	M3.5	3.4e-06	2.4e-06	< 2.5
324b	HD75732B	M4	2.2e-06	1.7e-06	< 2.5
1125	46655	M3.5	7.4e-07	5.9e-07	< 2.5
353	46769	M0	1.1e-05	7.9e-06	< 2.5
357	47103	M2.5	7.1e-07	5.1e-07	< 2.5
361	47513	M1.5	9.6e-06	6.5e-06	< 2.5
362	47650	M3	1.1e-05	7.6e-06	< 2.5
373	48714	M0	1.7e-05	1.1e-05	< 2.5
382	49986	M1.5	1.5e-05	1.0e-05	< 2.5
390	51007	M1	1.4e-05	9.6e-06	< 2.5
393	51317	M2	4.8e-06	3.5e-06	< 2.5
402	53020	M4	2.7e-06	2.0e-06	< 2.5
406	-	M6	3.2e-05	2.2e-05	< 2.5
408	53767	M2.5	2.8e-06	2.2e-06	< 2.5
411	54035	M2	1.4e-06	1.0e-06	< 2.5
412a	54211	M0.5	1.0e-06	7.5e-07	< 2.5

Table 1—Continued

GL	HIP/other	Type	L_h/L_{bol}	L_k/L_{bol}	$v \sin i$ (km/s)
413.1	54532	M2	2.8e-06	2.0e-06	< 2.5
414b	HD97101b	M1.5	1.0e-05	7.4e-06	< 2.5
424	55360	M0	6.8e-06	4.7e-06	< 2.5
433	56528	M1.5	3.9e-06	2.9e-06	< 2.5
1148	57050	M4	1.4e-06	1.0e-06	< 2.5
436	57087	M2.5	1.8e-06	1.4e-06	< 2.5
445	57544	M3.5	5.8e-07	5.1e-07	< 2.5
447	57548	M4	1.3e-06	9.0e-07	< 2.5
450	57802	M1	1.4e-05	9.5e-06	< 2.5
465	60559	M2	4.5e-07	3.7e-07	< 2.5
486	62452	M3.5	5.5e-07	4.5e-07	< 2.5
514	65859	M0.5	8.0e-06	5.7e-06	< 2.5
526	67155	M1.5	4.9e-06	3.6e-06	< 2.5
536	68469	M1	9.5e-06	6.4e-06	< 2.5
552	70865	M2	4.8e-06	3.3e-06	< 2.5
553.1	70975	M3.5	3.8e-07	1.5e-07	< 2.5
555	71253	M4	1.2e-06	8.8e-07	< 2.5
9492	71898	M3	1.4e-06	1.1e-06	< 2.5
569a	72944	M2	3.4e-05	2.4e-05	< 2.5
570b	73182	M1	1.5e-05	1.0e-05	< 2.5
581	74995	M3	6.0e-07	3.6e-07	< 2.5
617b	HD147379B	M3	3.5e-06	2.5e-06	< 2.5
625	80459	M1.5	2.4e-06	1.8e-06	< 2.5
628	80824	M3.5	1.3e-06	1.0e-06	< 2.5
649	83043	M1	1.3e-05	8.8e-06	< 2.5
655	83762	M3	1.6e-06	1.2e-06	< 2.5
3992	84099	M3.5	1.7e-06	1.2e-06	< 2.5
667c	-	M1.5	2.7e-06	2.1e-06	< 2.5
671	84790	M2.5	9.7e-07	7.8e-07	< 2.5
678.1a	85665	M0	9.4e-06	6.4e-06	< 2.5
687	86162	M3	1.6e-06	1.1e-06	< 2.5

Table 1—Continued

GL	HIP/other	Type	L_h/L_{bol}	L_k/L_{bol}	$v \sin i$ (km/s)
686	86287	M1	5.1e-06	3.7e-06	< 2.5
694	86776	M2.5	3.6e-06	2.5e-06	< 2.5
2130a	86961	M2	1.3e-05	8.7e-06	< 2.5
699	87937	M4	6.2e-07	4.5e-07	< 2.5
701	88574	M1	7.0e-06	5.0e-06	< 2.5
4048a	LHS462	M3	1.1e-06	8.2e-07	< 2.5
4062	G205-028	M3.5	2.5e-06	1.8e-06	< 2.5
4063	-	M3.5	2.9e-06	2.2e-06	< 2.5
4070	91699	M3	8.8e-07	6.4e-07	< 2.5
725a	91768	M3	5.7e-07	5.2e-07	< 2.5
725b	91772	M3.5	9.7e-07	7.1e-07	< 2.5
745a	93873	M1.5	-	-	< 2.5
745b	93899	M2	1.3e-07	-	< 2.5
4098	G207-019	M3	8.2e-07	6.8e-07	< 2.5
752a	94617	M2.5	4.7e-06	3.4e-06	< 2.5
793	101180	M2.5	6.2e-06	4.5e-06	< 2.5
806	102401	M1.5	6.4e-06	4.6e-06	< 2.5
809	103096	M0.5	1.2e-05	7.9e-06	< 2.5
821	104432	M1	7.6e-07	1.1e-06	< 2.5
846	108782	M0	1.7e-05	1.1e-05	< 2.5
849	109388	M3.5	2.2e-06	1.6e-06	< 2.5
851	109555	M2	1.4e-05	1.1e-05	< 2.5
860a	110893	M3	1.2e-06	8.9e-07	< 2.5
876	113020	M4	1.6e-06	1.3e-06	< 2.5
880	113296	M1.5	1.1e-05	7.5e-06	< 2.5
887	114046	M0.5	9.3e-06	6.0e-06	< 2.5
891	114411	M2	3.9e-06	2.8e-06	< 2.5
4333	115332	M4	2.1e-06	1.7e-06	< 2.5
895	115562	M1	1.9e-05	1.3e-05	< 2.5
905	-	M5	3.1e-06	2.4e-06	< 2.5
908	117473	M1	2.8e-06	2.3e-06	< 2.5

Table 1—Continued

GL	HIP/other	Type	L_h/L_{bol}	L_k/L_{bol}	v sin i (km/s)

Note. — Listed for our sample are the GL number, HIP number (or other name, in a few instances where either no HIP number exists or another name is in very common use), spectral type, L_h/L_{bol}, L_k/L_{bol}, and our determination of v sin i.

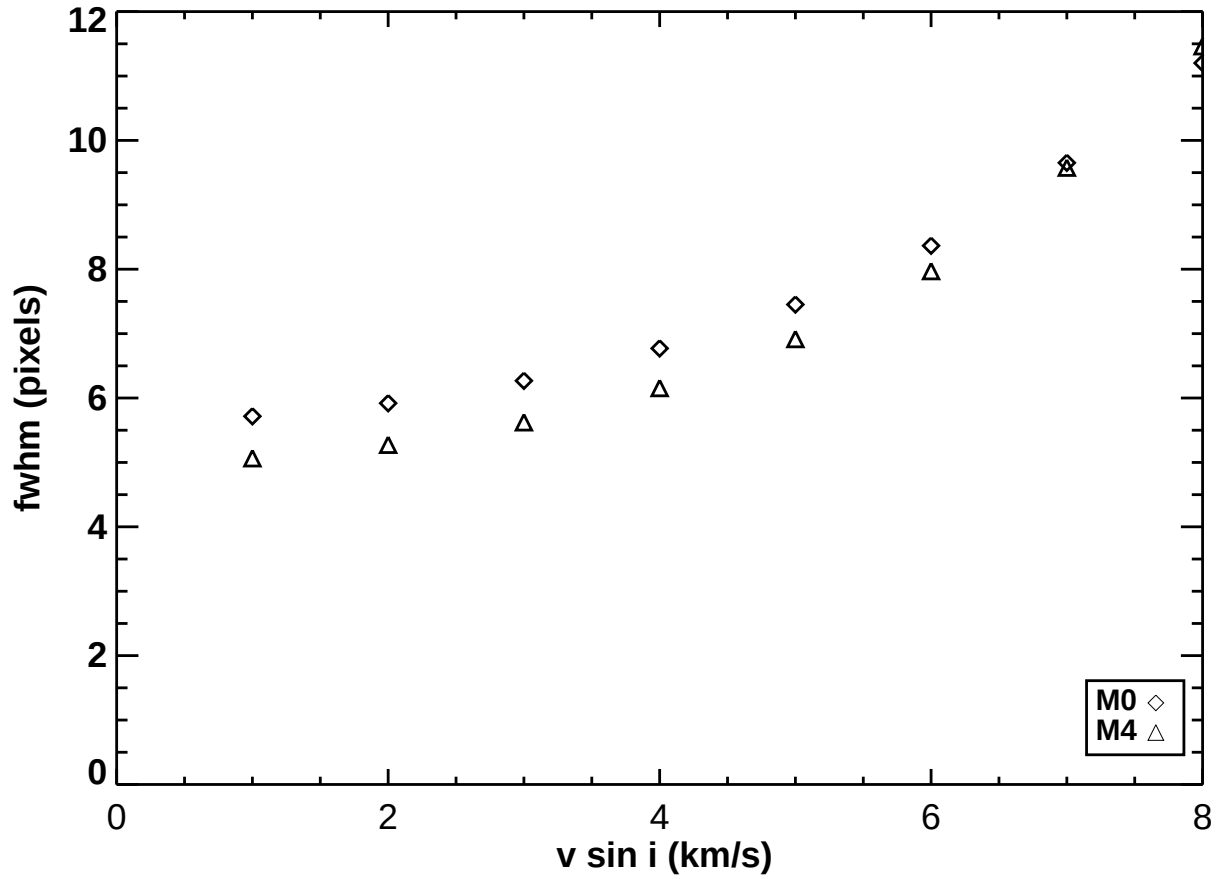

Fig. 1.— Full-width at half maximum (FWHM) of the cross-correlation function (XCF) between slowly rotating template stars and rotationally-broadened versions of the same spectra, for two different spectral types (indicated).

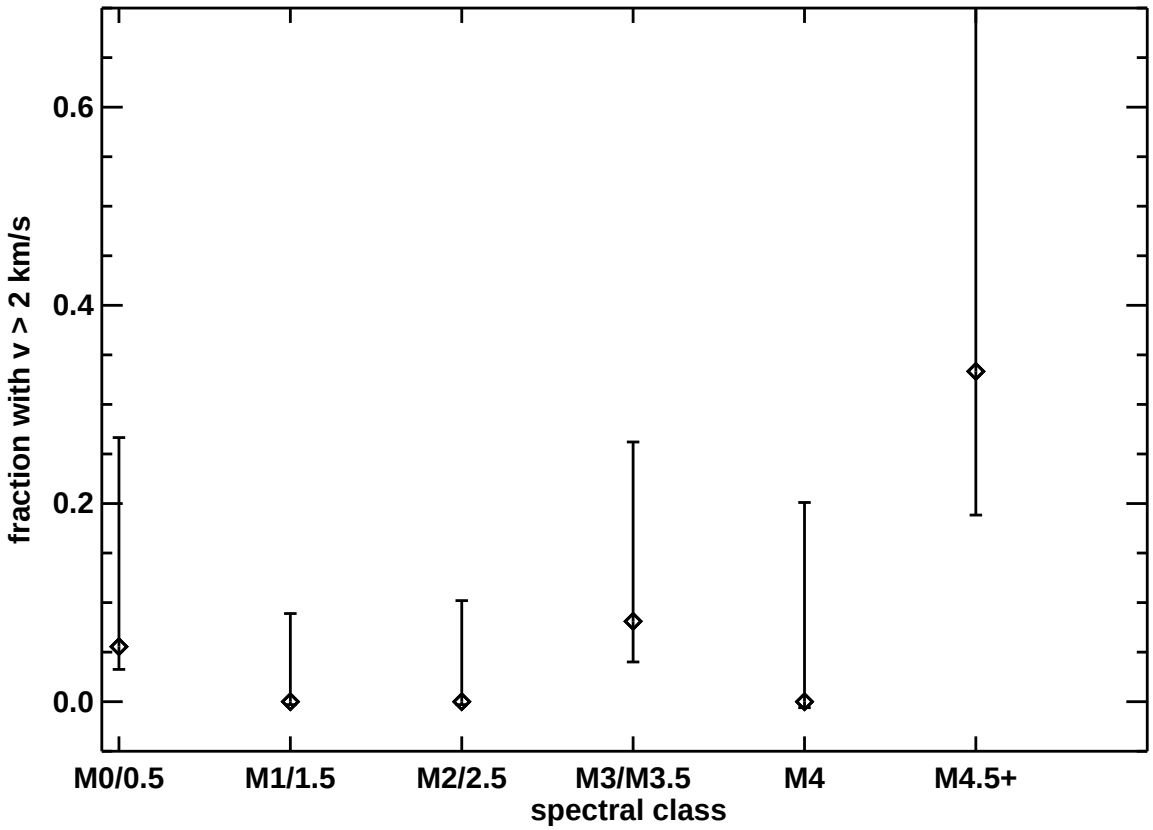

Fig. 2.— Fraction of stars detectably rotating (above a threshold $v \sin i \approx 2.5$ km s^{-1}) as a function of spectral type. The error bars shown are 1.5-σ errors for a binomial distribution in each mass bin.

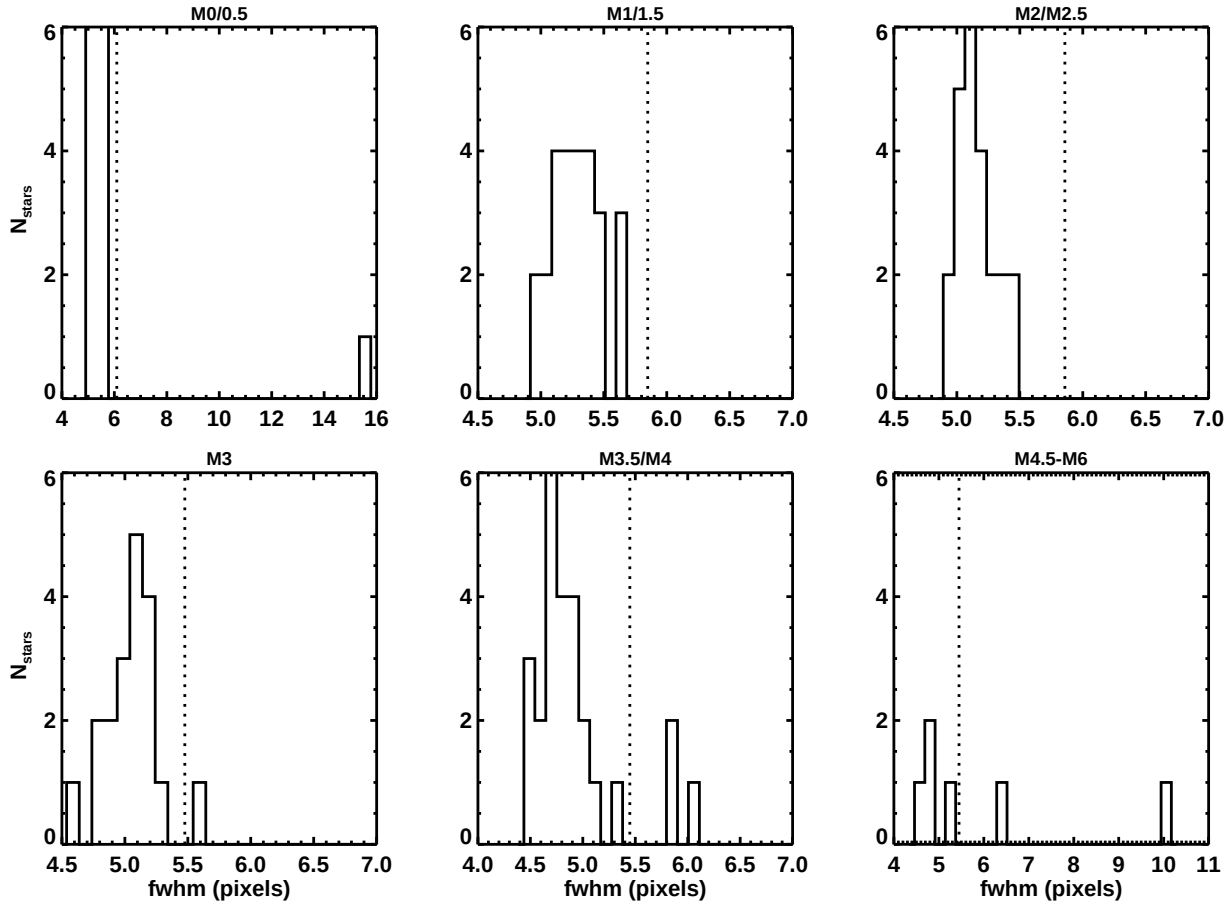

Fig. 3.— Histograms of XCF FWHMs for observations in different spectral class bins. Also shown as a vertical dashed line is the FWHM measured for a rotationally-broadened template (with v sin i = 2.5 km s^{-1}) in each spectral class. Claimed detections of rotation are generally significant outliers in the FWHM distribution.

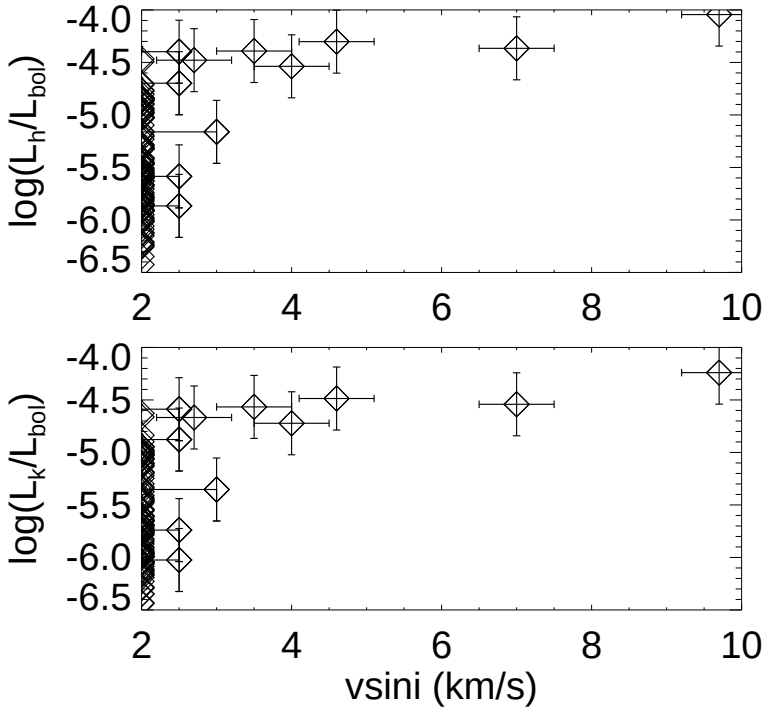

Fig. 4.— Luminosity in the Ca II H and K chromospheric emission lines, normalized to the bolometric luminosity, as a function of v sin i.

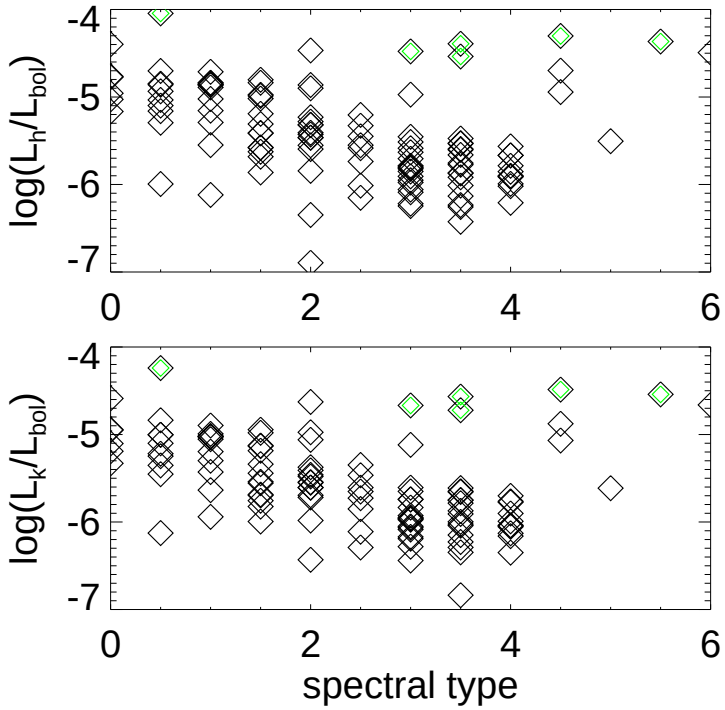

Fig. 5.— Luminosity in the Ca II H and K chromospheric emission lines, normalized to the bolometric luminosity, as a function of spectral type. Stars in which we have detected rotation are overplotted in green.